Low Noise Multiquantum Well DAR IMPATT Diodes Based On Si_XGe_{1-X}/Si

Suranjana Banerjee

Assistant Professor

Department of Electronics, Dum Dum Motijheel College, Kolkata-700074

Abstract **- A Multiquantum Well (MQW) Si_xGe_{1-x}/Si DAR (Double Avalanche Region) IMPATT (Impact Avalanche Transit Time) diode as a high power-high efficiency-low noise source at W-band is proposed in this paper. The RF power, conversion efficiency and noise of the device are optimized with respect to number of quantum wells and Ge mole fraction. The proposed device delivers peak power of 2.7 W, conversion efficiency of 7.5% and noise measure of 25 dB when the number of wells in the MQW structure is four and mole fraction of Ge is 0.3. The admittance plots of the device exhibit distinct negative conductance bands for three different (0.1, 0.2 and 0.3) mole fractions of Ge. An upward shift of optimum frequency is observed with increasing Ge mole fraction. The noise measure of the device decreases with increasing mole fraction of Ge and decreasing current.**

Keywords *- Multiquantum Well; DAR IMPATT; W-band; Mole fraction of Ge, negative conductance*

I. INTRODUCTION

Silicon IMPATT device with Double Drift Region (DDR) (n^+-n-p-p^+) structure having a central avalanche region between two drift regions is well established as high-power - high-efficiency source at W-band (75-110 GHz) [1,2]. However, at higher bias current, the effect of mobile space charge restraints the RF power and efficiency of the device [3]. Double Avalanche Region (DAR), n^+-p-υ-n-p^+ IMPATT structure [4] overcomes this limitation where a nearly intrinsic drift region (ν-region) is interspaced between two avalanche zones near the two edges of the active layer. The space charge effect is almost cancelled in the central drift layer (ν-region) due to the opposite drift of electrons and holes generated from two avalanche zones. The effect of mobile space charge at very high bias current density almost cancels in the central drift layer of DAR structure as reported in [4], quite different from DDR structure resulting in high power at high bias current level from DAR IMPATTs.

Avalanche noise in IMPATT diode is another prime concern as it is very high (around 40 dB) in DDR IMPATTs. DAR device with two avalanche zones will therefore produce even more noise.

However, heterojunction (HT) IMPATTs show improved noise performance as compared to homojunction (HM) IMPATTs. HT DDR IMPATTs provide higher RF power with higher DC to RF conversion efficiency and less noise as compared to HM DDR IMPATTs as reported [5 - 8]. This is due to larger peak field at the junction and sharper breakdown in HT IMPATTs. Therefore, the author proposes a

heterostucture multiquantum well (MQW) DAR IMPATT based on Si_xGe_{1-x}/Si as a high power and low noise RF source. The large signal admittance characteristics of the proposed device are obtained and compared with that of HM Si DAR device at mm-wave W-band frequency. The mole fraction, x of Ge and the number of quantum wells in the proposed structure are varied to optimize the RF power, conversion efficiency and the noise measure of MQW DAR IMPATT device.

II. DEVICE STRUCTURE

One dimensional MQW DAR (n^+ p ν n p^+) IMPATT device structure based on Si_xGe_{1-x}/Si is shown in Fig.1. Equal number of quantum wells is incorporated within the p and n layers of the device. The RF power, conversion efficiency and noise of the proposed device are optimized by varying the number of quantum wells. The well width of Si_xGe_{1-x} and the barrier width of Si are assumed to be equal and their thicknesses are varied according to the number of wells in the MQW structure. Three mole fractions of Ge (0.1, 0.2 and 0.3) are considered for the present study. The drift layer width, x_d is basically the width of ν-layer and the avalanche layer width are x_{Ap} and x_{An} respectively. The doping concentrations and thicknesses of different layers of the device are designed for operation at W-band by using the design criterion of Sze and Ryder [9]. The design parameters are listed in Table 1.

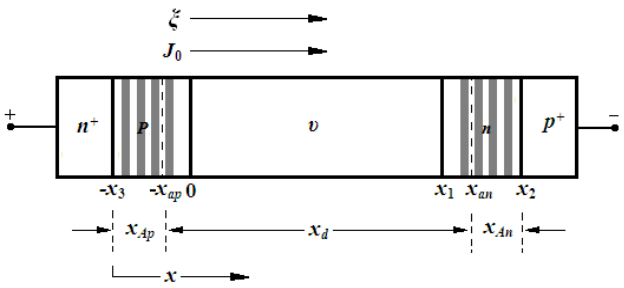

Fig. 1. One-dimensional model of MQW DAR IMPATT diode

TABLE 1: STRUCTURAL AND DOPING PARAMETERS

Design parameters	Value
n-layer width, W_n (μm)	0.160
ν-layer width, x_d (μm)	1.500
p-layer width, (μm)	0.150
n^+layer width, (μm)	0.001
p^+layer width, (μm)	0.001
n -doping concentration,N_D ($\times 10^{23}$ m^{-3})	2.500
ν-layer concentration, N_i ($\times 10^{23}$ m^{-3})	0.010
p-doping concentration, N_A ($\times 10^{23}$ m^{-3})	2.500
n^+ doping concentration, N_{n+} ($\times 10^{25}$ m^{-3})	5.000
P^+ doping concentration ,N_{p+} ($\times 10^{25}$ m^{-3})	2.700
Junction diameter, D_j (μm)	45.000

III. LARGE SIGNAL MODEL AND SIMULATION METHOD

The large signal simulation of the proposed MQW DAR IMPATT diode is carried out using Non Sinusoidal Voltage Excitation (NSVE) model [10]. Simultaneous numerical solution of time and space dependent Poisson's equation, continuity equation and current density equation is carried out subject to the appropriate field and current boundary conditions at the depletion layer edges. Finite difference method (FDM) [11] is used for numerical analysis.

The non-sinusoidal voltage waveform is given by

$$v_{rf}(t) = V_B \sum_{p=1}^{n} (m_x)^p \sin(2p\pi f_d t) \qquad (1)$$

where m_x is the voltage modulation factor or the RF voltage swing. It is defined as the ratio of the magnitude of RF voltage to the DC breakdown voltage (V_B). The fundamental component of RF voltage corresponds to p=1 and can be expressed as $v_{rf1}(t) = m_x V_B \sin(2\pi f_d t)$ where the fundamental frequency, f_d is equal to the design frequency. The number of harmonics present in the voltage waveform is $(n - 1)$.
When a time varying voltage, $v_{rf}(t)$ is applied, the current response of the device is $J_t(t) = J_0 + j_t$ where J_0 is the bias current density and j_t is the terminal current.

The DC parameters like peak electric field at the junction, ξ_P, breakdown voltage, V_B, avalanche zone voltage, V_A, and avalanche zone width, x_A of the proposed device are obtained from DC simulation where the device equations are made time independent but space dependent. Here, the RF voltage, V_{RF} = zero and therefore $m_x = 0$.

The large signal simulation is then carried out using the aforementioned DC parameters as input and increasing the voltage modulation factor, m_x in small steps of Δm_x where Δm_x = 0.05 (5%). The large-signal program is initially run for the first complete cycle i.e. $0 \le \omega t \le 2\pi$. The oscillation stability is tested by running the program over consecutive cycles. The amplitude of the fundamental component of RF voltage is $V_{RF} = m_x V_B$.. The terminal voltage and current waveforms, $V_t(t)$ vs. t and $J_t(t)$ vs. t are obtained from the snapshots of electric field, [$\xi(x,t)$ vs. x],terminal voltage, [$V(x,t)$ vs. x], electron and hole current densities,[$J_n(x,t)$ vs. x and $J_p(x,t)$ vs. x] at different phase angles of a full oscillation cycle. Fourier analysis of terminal voltage and current waveforms over a full cycle provides the necessary frequency domain information. The large-signal parameters of the device are obtained for different voltage modulation factors. The device admittance, $Y_D(\omega)$ is calculated from the ratio of terminal current to the applied voltage in frequency domain. The normalized negative conductance, $G(\omega)$ and susceptance, $B(\omega)$ of the device with respect to the junction area, A_j of the device are computed from the real and imaginary parts of device admittance. If the large signal admittance be $Y_D(\omega)$, then the corresponding impedance is given by

$$Z_D(\omega) = \frac{1}{Y_D(\omega)} = \frac{1}{[G(\omega) + jB(\omega)]A_j} = Z_R(\omega) + iZ_X(\omega) \qquad (2)$$

where $Z_R(\omega)$ and $Z_X(\omega)$ are the negative resistance and reactance of the device, given by

$$Z_R(\omega) = \frac{G(\omega)}{[G(\omega)^2 + B(\omega)^2]A_j}$$
$$Z_X(\omega) = \frac{-B(\omega)}{[G(\omega)^2 + B(\omega)^2]A_j} \qquad (3)$$

The large signal output power is calculated from

$$P_{RF} = \frac{1}{2}(V_{RF})^2 |G_p| A_j \qquad (4)$$

where, V_{RF} is the RF voltage and $|G_p|$ is the normalized peak negative conductance at the optimum frequency. The DC to RF conversion efficiency is calculated from

$$\eta_L = \frac{P_{RF}}{P_{DC}} \qquad (5)$$

The DC input power is given by $P_{DC} = J_0 V_B A_j$, whereJ_0 is the DC bias current density.

The large signal admittance characteristics [conductance (G) - susceptance (B) plots] for MQW DAR IMPATT device are then obtained for a particular voltage modulation, m_x and RF

voltage. These characteristics provide useful large signal parameters of the proposed device such as optimum frequency, f_p , avalanche resonance frequency, f_a , peak negative conductance, G_p, and susceptance, B_p , device negative resistance, Z_R , Quality factor, Q_p , power output P_{RF} and conversion efficiency, η_L.

IV. NOISE SIMULATION TECHNIQUE

The impact ionization phenomenon causes random generation of electron-hole pairs which produces avalanche noise, the prime source of noise in IMPATT devices. This results in random fluctuation of DC current and electric field which may be regarded as small-signal components of the respective parameters in absence of time varying voltage across the device. The noise analysis can therefore be carried out under open circuit condition of the device in which time varying applied voltage is absent. Let us assume that a noise source, $\gamma(x')$ located at x' in the depletion layer of IMPATT diode produces the noise field where $\gamma(x')$ is given by

$$\gamma(x') = \alpha_n(x')v_n(x')n(x') + \alpha_p(x')v_p(x')p(x') \quad (6)$$

In Eqn. (6), $\alpha_n(x')$ and $\alpha_p(x')$ are the impact ionization rate of electrons and holes , $v_n(x')$ and $v_p(x')$ are the drift velocity of electrons and holes and $n(x')$, $p(x')$ are the electron, hole concentration at the space point x' in the active region of the device.

The small-signal noise field due to the noise source $\gamma(x')$ is expressed as $e_n(x,x') = e_{nr}(x,x') + je_{ni}(x,x')$. Two second order differential

equations in the real ($e_{nr}(x,x')$) and imaginary ($e_{ni}(x,x')$) parts of the noise field $e_n(x,x')$ are formed by using Gummel-Blue method [12]. Simultaneous numerical solution of the differential equations for the real and imaginary parts of noise field is carried out subject to appropriate boundary conditions at the depletion layer edges by using Runge-Kutta method. The solution provides the distribution of noise field in the depletion layer of the device.

The simulation is carried out by taking the noise source $\gamma(x')$ first at one boundary of the active region, $x = 0$ and then the source is shifted to the next space point, $(x+\Delta x)$. The procedure is repeated till the other boundary ($x = W$) is reached. Terminal voltage $v_t(x')$ due to the noise source at x' is obtained from the numerical integration of noise field, $e_n(x,x')$ over the entire depletion layer (i.e. from $x = 0$ to $x = W$). Thus

$$v_t(x') = \int_{x=0}^{x=W} e_n(x,x')dx \quad (7)$$

The transfer impedance of the device ($z_t(x')$) is obtained from the ratio of terminal voltage, $v_t(x')$ to the mean noise current, $i_n(x')$ produced within the space step, $\Delta x'$ due to the presence of noise source.

The mean-square noise voltage is calculated from

$$\langle v_n^2 \rangle = 2q^2.df.A_j \int |z_t(x')|^2 \gamma(x')dx' \quad (8)$$

The effective junction area, A_j is obtained from the junction diameter given in Table 1, considering a circular mesa structure of the MQW DAR device. The noise spectral density i.e. the mean-square noise voltage per bandwidth $[\langle v_n^2 \rangle / df]$ is then computed. The noise measure (M_N) of the device [13] is obtained from the following equation

$$M_N = \frac{\langle v_n^2 \rangle / df}{4k_B T_j(-Z_R - R_S)} \quad (9)$$

where, k_B is the Boltzmann constant, T_j is the junction temperature in degree Kelvin (K) and R_S is the positive parasitic series resistance of the device.

V. RESULTS AND DISCUSSIONS

i)*Admittance characteristics:* The large signal admittance characteristics of the proposed device are obtained for three mole fractions of Ge (x=0.1, 0.2 and 0,3) at a bias current density of 5.0×10^{8} A m^{-2}, taking 50% voltage modulation. Fig.2 shows these characteristics along with those of conventional Si DAR IMPATT diode for the sake of comparison. It is observed that the admittance (G – B) plots of the proposed device exhibit four distinct negative conductance frequency bands separated by positive conductance for all three mole fractions of Ge. Similar feature is observed in the plots of normal Si DAR IMPATT device. The four frequency bands are (i) band-1 (62-87 GHz) (ii) band-2 (105-130 GHz) (iii) band-3 (149-172 GHz) and (iv) band-4 (192-215 GHz). This is a unique feature of admittance characteristics of DAR IMPATT diode which is not observed in SDR or DDR IMPATT diode. This has the advantage of using DAR IMPATTs designed at a lower mm-wave frequency band to operate at higher mm-wave frequency band. It is interesting to observe from Fig. 2 that the optimum frequency at which the negative conductance attains a peak value is slightly higher in MQW DAR IMPATTs than in normal DAR Si IMPATTs for all the four bands. An upward shift of optimum frequency by 1 to 3 GHz is observed with increasing Ge mole fraction. This feature of MQW DAR IMPATT device can be used advantageously in mm-wave systems with respect to frequency tuning.

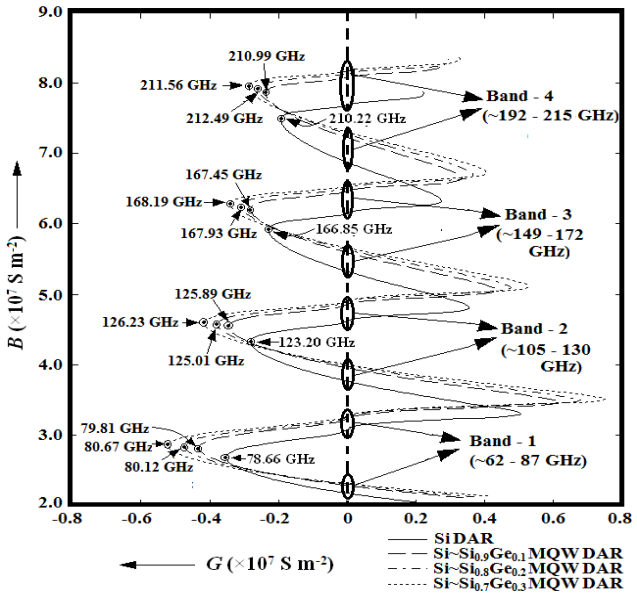

Fig. 2. Large-signal admittance characteristics (showing four distinct frequency bands 1-4 of operation) of DAR Si IMPATT and MQW Si~$Si_{1-x}Ge_x$ DAR IMPATTs (x = 0.1, 0.2 and 0.3) with 4 quantum wells (N = 4) at a bias current density of J_0 = 5.0×10^{8} A m^{-2} and voltage modulation of 50%

ii)*Large signal power and conversion efficiency versus number of wells in the MQW DAR IMPATT structure:* Fig. 3(a) shows the variation of large signal output power of MQW DAR IMPATT device based on Si~$Si_{0.7}Ge_{0.3}$ with the number of quantum wells in the MQW structure. It is observed that the output power increases with the increase of the number of quantum wells, reaches a maximum value when the number of wells is four and then decreases for each operating frequency band. Fig. 3(b) shows the variation of conversion efficiency of the device with the number of quantum wells in the MQW structure. The nature of variation of conversion efficiency with the number of wells is similar to that of RF output power as shown in Fig. 3 (a). The conversion efficiency of the device attains peak value for each band when the number of quantum wells is also four. Thus, the number of wells required in the structure is four to maximise both RF power and conversion efficiency. The peak output power is highest (2.7 W) for band 1 and decreases gradually from

band 1 to band 4 for a fixed number of wells. The peak conversion efficiency is also highest (7.5%) for band 1 and lowest for band 4 (4.2%) for a fixed number of wells.

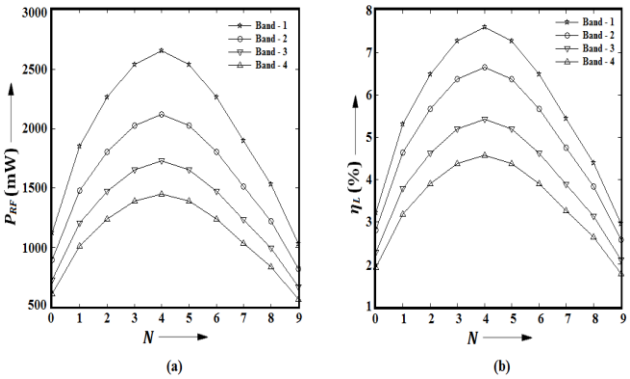

Fig. 3. Variations of (a) RF power output and (b) DC to RF conversion efficiency of MQW DAR IMPATT diode based on Si~$Si_{0.7}Ge_{0.3}$ material system at different frequency bands with number of quantum wells for the bias current density of $J_0 = 5.0\times10^8$ A m^{-2}.

iii)*Noise measure(NM)-frequency plot:* Fig.4 shows the noise measure-frequency plots of the proposed MQW DAR Si~$Si_{1-x}Ge_x$ IMPATTs for three Ge mole fractions (x = 0.1, 0.2 and 0.3) with four quantum wells at bias current densities of 0.5x10^8, 1.0x10^8 and 5.0 x10^8 Am^{-2}. The plots of normal DDR and DAR Si IMPATTs are also shown for the sake of comparison. Normal Si DAR shows the highest NM at a particular bias current followed by DDR Si and it is lowest in the proposed MQW DAR Si~$Si_{1-x}Ge_x$ device. The NM decreases with decreasing bias current density and increasing Ge mole fraction for all three devices and attains a minimum level of 25 dB in MQW DAR Si~$Si_{0.7}Ge_{0.3}$ IMPATTs at a bias current density of 0.5×10^8A m^{-2}.

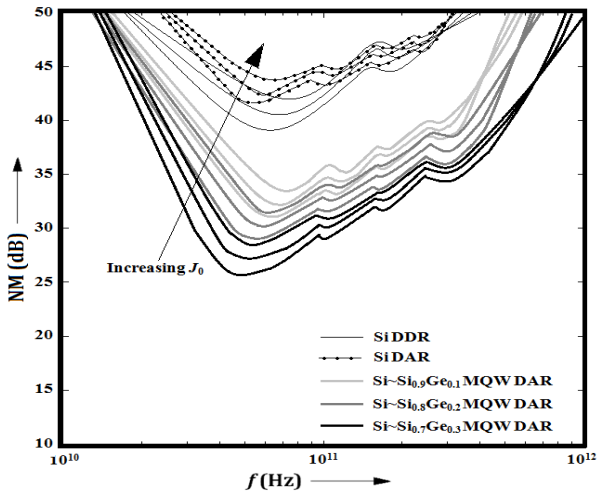

Fig. 4. Variations of noise measure with frequency for DDR Si IMPATT, DAR Si IMPATT and MQW DAR IMPATTs based on Si~$Si_{1-x}Ge_x$ material system (x = 0.1, 0.2 and 0.3) having number of quantum wells N = 4, at three different bias current densities

VI. CONCLUSION

The number of quantum wells and mole fraction of Ge are varied to optimize the output power, conversion efficiency and avalanche noise of a proposed Si ~$Si_{1-x}Ge_x$ based MQW DAR IMPATT device.

The device can operate at frequencies higher than the design frequency band as obvious from the G-B plots of the proposed device that manifest the fascinating feature of four negative conductance bands quite similar to those of normal DAR Si IMPATTs.

With variation of Ge mole fraction from 0.1 to 0.3 in the MQW structure, frequency chirping is observed by a few GHz which can be explored in frequency tuning application in mm-wave communication system.

A peak power of 2.5 W with peak conversion efficiency of 7.5% and low noise measure of 25 dB is obtained from the proposed device, when the number of quantum wells in the structure is four and mole fraction of Ge is 0.3. Thus, MQW DAR IMPATT device can be considered as a high power-high efficiency-low noise source that excels both normal DAR and DDR Si

IMPATTs. This source will find applications in millimeter wave communication system, tracking RADARs and missile guidance. So, the results presented in this paper will be beneficial for the development of MQW DAR IMPATTs for various civilian and defense applications at mm-wave frequency bands.

VII. REFERENCES

[1] T.T. Fong and H.J. Kuno, "MM-wave pulsed Impatt sources", *IEEE Trans. Microwave Theory and Tech.*, Vol. MTT-27, p.492 (1979).

[2] W. Behr and J.F. Luy, " High-Power operation mode of pulsed Impatt diodes", *IEEE Electron Dev. Lett.*, Vol. EDL-11, p.206 (1990).

[3] J.P. Banerjee, S.P. Pati and S.K. Roy, "Computer studies on the space charge dependence of avalanche zone width and conversion efficiency of single drift p^+nn^+ and n^+pp^+ Indium Phosphide Impatts*", Appl. Phys. A*, Vol. 35, p. 125 (1984).

[4] Dutta,D.N., Pati, S.P., Banerjee, J.P., Pal,B.B., Roy, S.P.: "Computer analysis of DC field and current density profiles of DAR Impatt diodes", *IEEE Trans. Electron Devices* **29**, 632–677 (1982).

[5] M. J. Bailey, "Hetrojunction IMPATT diodes", *IEEE Trans Electron Devices*, Vol.39, p.1829 (1992).

[6] J.C. De Jaeger, R. Kozlowski and G. Salmer, "High efficiency GaInAs/InP heterojunction", *IEEE Trans Electron Devices*, Vol. 30, Issue 7, p. 790-796 (1983).

[7] N.S Dogan, J,R. East, M. Elta and G.I. Haddad, "Millimeter wave heterojunction MITATT diodes", *IEEE Trans. Microwave Theory and Tech.*, Vol. MTT 35, p.1304 (1987).

[8] G.N. Dash and S.P. Pati, "Computer aided studies on the microwave characteristics of InP/GaInAs and GaAs/GaInAs heterostructure single drift region impact avalanche transit didoes", *J. Phys. D. Appl. Phys.*, Vol.27, p.1719 (1994).

[9] [11] S.M. Sze and R.M. Ryder, "Microwave avalanche didoes", *Proc. IEEE (Lett.)*, vol. 59, p.1140 (1971).

[10] A. Acharyya, S. Banerjee and J. P. Banerjee, " Large signal simulation of 94 GHz pulsed DDR Silicon IMPATTs including the temperature transient effect", *Radioengineering* [Czech and Slovak], Vol. 21, no. 4, pp. 1218-1225 (2012).

[11] J. Douglas, and Y. Yuan, "Finite difference methods for the transient behavior of a semiconductor device," IMA Preprint Series#286, *Institute for Mathematics and Its Applications, University of Minnesota, Minnesota* (1987).

[12] H. K. Gummel, and J. L. Blue, "A small-signal theory of avalanche noise in IMPATT diodes," *IEEE Trans. on Electron Devices*, vol. 14, pp. 569-580 (1967).

[13] Suranjana Banerjee, Aritra Acharyya and J. P. Banerjee, "Noise Performance of Heterojunction DDR MITATT Devices Based on $Si{\sim}Si_{1-x}Ge_x$ at W-Band," *Active and Passive Electronic Components [USA]*, vol. 2013, pp. 1-7 (2013).